Biochimica et Biophysica Acta 1802 (2010) 572–581

Contents lists available at ScienceDirect

Biochimica et Biophysica Acta

journal homepage: www.elsevier.com/locate/bbadis

A novel germline mutation in Peroxisome Proliferator-Activated Receptor γ gene associated with large intestine polyp formation and dyslipidemia

D. Capaccio [a,c,1], A. Ciccodicola [b,1], L. Sabatino [a,c], A. Casamassimi [b], M. Pancione [a], A. Fucci [a], A. Febbraro [d], A. Merlino [e], G. Graziano [a], V. Colantuoni [a,c,*]

[a] Department of Biological and Environmental Sciences, University of Sannio, Via Port'Arsa, 11, 82100 Benevento, Italy
[b] Institute of Genetics and Biophysics, "A. Buzzati-Traverso" CNR, Via P. Castellino, 113, 80131 Napoli, Italy
[c] Department of Biochemistry and Medical Biotechnologies, University of Naples "Federico II", Via S. Pansini, 5, 80131 Napoli, Italy
[d] Fatebenefratelli Hospital, Division of Medical Oncology, Viale Principe di Napoli, 82100 Benevento, Italy
[e] Department of Chemistry, University of Naples "Federico II", Monte S. Angelo, 80100 Napoli, Italy

ARTICLE INFO

Article history:
Received 24 November 2009
Received in revised form 7 January 2010
Accepted 19 January 2010
Available online 1 February 2010

Keywords:
Peroxisome Proliferator-Activated Receptor
Loss-of-function mutation
Colorectal cancer
Dyslipidemia

ABSTRACT

We report a novel *PPARG* germline mutation in a patient affected by colorectal cancer that replaces serine 289 with cysteine in the mature protein (S289C). The mutant has impaired transactivation potential and acts as dominant negative to the wild type receptor. In addition, it no longer restrains cell proliferation both in vitro and in vivo. Interestingly, the S289C mutant poorly activates target genes and interferes with the inflammatory pathway in tumor tissues and proximal normal mucosa. Consistently, only mutation carriers exhibit colonic lesions that can evolve to dysplastic polyps. The proband presented also dyslipidemia, hypertension and overweight, not associated to type 2 diabetes; of note, family members tested positive for the mutation and display only a dyslipidemic profile at variable penetrance with other biochemical parameters in the normal range. Finally, superimposing the mutation to the crystal structure of the ligand binding domain, the new Cys289 becomes so closely positioned to Cys285 to form an S–S bridge. This would reduce the depth of the ligand binding pocket and impede agonist positioning, explaining the biological effects and subcellular distribution of the mutant protein. This is the first *PPARG* germline mutation associated with dyslipidemia and colonic polyp formation that can progress to full-blown adenocarcinoma.
© 2010 Elsevier B.V. All rights reserved.

1. Introduction

Peroxisome Proliferator-Activated Receptors (PPARs) are ligand-dependent transcription factors belonging to the nuclear hormone receptor superfamily [1]. Three different isoforms, α, β/δ and γ have been isolated so far, each encoded by a distinct gene. *PPARG* (MIM# 20601487) generates four mRNAs by alternate splicing and differential promoter usage that are translated into two proteins, γ1 and γ2 that differ for 28 additional amino acids at the N-terminus of the γ2 protein [2]. The two isoforms have different expression patterns: PPARγ2 is mostly expressed in adipose tissue, whereas PPARγ1 is expressed in colon, monocytes/macrophages and at lower levels in other tissues including muscle and liver. PPARγ integrates the control of energy, lipid and glucose homeostasis. Moreover, it plays a pivotal role in adipogenesis and in the differentiation pathways of many epithelial cells [1–4]. Since *PPARG* isolation and characterization, several heterozygous mutations have been described and correlated with distinct clinical phenotypes [5]. A frameshift mutation in *PPARG* exon 3, coding for the DNA binding domain of the receptor, results into a truncated, inactive form of the protein [6]. Missense and nonsense mutations at different codons of exons 5 affect the amino acid residues that contribute to the ligand binding pocket formation and coactivator recruitment [5]. These mutants have impaired ability to bind selective agonists, significant reduction in transcriptional activity and some of them exert a dominant negative effect vs. the wild type receptor [5 and references therein]. Human subjects bearing some of these loss-of-function mutations present type 2 diabetes and several features of the metabolic syndrome (such as insulin resistance, dyslipidemia, and hypertension) accompanied by partial lipodistrophy [5]. A single *PPARG* gain-of-function mutation, P113G, has been reported. It prevents phosphorylation of the neighbouring serine 112 by growth factors via the MAP kinases cascade, thus stimulating receptor activity [7].

Interestingly, some of the *PPARG* loss-of-function mutations have been found in sporadic colorectal cancers, linking this gene's alterations to colon tumorigenesis [6,8]. PPARγ activation in several tumors and tumor cell lines by specific agonists results in induction of

Abbreviations: PPAR, Peroxisome Proliferator-Activated Receptors; CRC, colorectal cancer; LOH, loss of heterozygosity; *APC*, adenomatous poliposis coli

* Corresponding author. Department of Biological and Environmental Sciences, University of Sannio, Via Port'Arsa, 11, 82100 Benevento, Italy.
E-mail address: colantuoni@unisannio.it (V. Colantuoni).

[1] These two authors contributed equally to this work.

0925-4439/$ – see front matter © 2010 Elsevier B.V. All rights reserved.
doi:10.1016/j.bbadis.2010.01.012

apoptosis, cell cycle progression block or stimulation of terminal differentiation [9]. PPARγ is, therefore, considered a tumor suppressor [6,8], a role that has been questioned because of the conflicting results reported [8 and references therein]. In support to the anti-proliferative function, a new PPARγ isoform lacking the ligand binding domain has been found in colorectal cancer, shown to interfere with wild type receptor and to stimulate cell proliferation [10].

In an attempt to correlate *PPARG* mutations with tumorigenesis, we screened a series of colorectal cancers and we report here a novel germline mutation in a patient with late tumor onset, dyslipidemia, hypertension and high body mass index (BMI) with normal blood glucose and insulin levels. Family members, tested positive for the mutation, presented colonic lesions that can evolve with time to dysplastic polyps along with different arrays of lipid derangements. This is the first *PPARG* germline mutation, linked to dyslipidemia and large intestine polyps, without features of type 2 diabetes. These and other aspects of *PPARG* structure and function are discussed.

2. Materials and methods

2.1. DNA, RNA extraction and RT-PCR assay

DNA was extracted from tumor tissues and normal matched mucosa as previously reported [10]. RNA was extracted from tissues and cell lines by Trizol™ (Invitrogen, Carlsbad, CA). For cDNA synthesis, random primed double-stranded cDNA was synthesized using Superscript III (Invitrogen, Carlsbad, CA). The specificity of each oligonucleotide pair used was verified with the BLAST Program, whereas the amplification conditions were experimentally determined. PCR products were sequenced with the Big Dye Reaction Kit (Applied Biosystem, Foster City, CA) and a 3100 ABI Prism automated sequencer (Applied Biosystem, Foster City, CA). To synthesize PPARγ cDNA by RT-PCR, we used the following primers: PPARγ exon 1 forward: 5′-TCTCTCCGTAATGGAAGA CC-3′; exon 3 reverse: 5′-GCATTATGAGACATCCCCAC-3′; exon 2 forward: 5′-ACT CAGCTCTA-CAATAAGCCTCATGAA-3′; and exon 6 reverse: 5′-CTAGTACAAGTCCTT GTAGATCT-3′. Nucleotide numbering was performed based on the reference cDNA sequence (GenBank NM_138712.3), where +1 corresponded to the nucleotide A of ATG, the translation initiation codon. We subdivided the cDNA obtained in two halves, that were PCR amplified and automatically sequenced using exon 1–exon 3 and exon 2–exon 6 oligonucleotide primer pairs, respectively. To confirm that the mutation detected in the cDNA was present also at the DNA level, we PCR amplified and directly sequenced exon 5 from the DNA extracted from tumor and peripheral blood. The primers used were: exon 5 forward: 5′-GAATTCCTTAATGATGGGAG-3′; and reverse: 5′-CAATAAATATTGCCAAGTCG-3′.

2.2. Expression vectors

S289C V290M and PPARγ cDNAs (used as controls) were cloned in a pcDNA3 based expression vector (Invitrogen, Carlsbad, CA) in-frame with a 5′-end FLAG epitope. The wild type and S289C mutant cDNAs were obtained by RT-PCR starting from total RNA extracted from tumor tissues. The V290M mutant cDNA, kindly provided by Prof. Chatterjee, V, K. Cambridge, UK, was transferred into the same vector. The V290M mutant has impaired transcriptional activity and acts as dominant negative to the wild type receptor [11,12]. The right insertion was determined by restriction enzyme map and the correct sequence by automated DNA sequencing of the plasmids.

2.3. Cell lines and transfections

Cos7, NIH-3T3 and LoVo cells (these latter are derived from a human colorectal carcinoma) were grown in Dulbecco's modified Eagle's media supplemented with 2 mM glutamine and 10% fetal calf serum in a 5% CO_2 humidified atmosphere at 37 °C. Cos7 and LoVo cells were transfected by Lipofectamine 2000 (Invitrogen, Carlsbad, CA), and NIH-3T3 cells by Fugene 6 (Roche, Mannheim, Germany). Where indicated, 16 h after transfection, troglitazone (Sigma-Aldrich, St. Louis, MO) dissolved in dimethylsulfoxide or the vehicle alone was added at the indicated concentrations and incubated for a further 24 h.

2.4. Transactivation assay

All transfections were carried out with a luciferase reporter gene under the transcriptional control of the herpes simplex thymidine kinase (TK) promoter fused to three copies of the PPRE derived from the Acyl-CoA oxidase gene (PPRE-TK-Luc) [6,10]. Expression vectors containing 5′FLAG-tagged-PPARγ and mutant cDNAs (50 or 100 ng) were transfected alone or in combination; fixed amount (250 ng) of the reporter gene were used in each experiment [10]. In all cases, 200 ng of the CMV-β galactosidase-containing plasmid were cotransfected to normalize for transfection efficiency. Forty-eight hours later, luciferase and β-galactosidase activity were determined on cell extracts and luciferase was normalized to β-galactosidase.

2.5. Colony-forming efficiency assay

The day after seeding, NIH-3T3 cells (10^5 cells/six-well plate) were transfected with 2 μg of the empty vector or the PPARγ and S289C mutant cDNAs containing plasmids by Fugene 6 (Roche, Mannheim, Germany). The cells were exposed to the Fugene–DNA complexes for 16–20 h and then split 1:10 in 100-mm plates in the G418 selection medium (600 μg/ml Geneticin, Invitrogen Carlsbad, CA). After 15 days, the plates were stained with Crystal Violet. Colony-forming efficiency was calculated by dividing the number of colonies obtained on plates transfected with the various PPARγ constructs by that obtained with the empty vector [13].

2.6. BrdUrd incorporation

NIH-3T3 were transfected with the various cDNA containing expression vectors. DNA synthesis was assayed by a 2-h pulse with 100 μM BrdUrd, and incorporation was monitored as reported [14] by using the *in situ* cell proliferation kit FLUOS (Roche, Mannheim, Germany).

2.7. Western blot analysis and antibodies

Western blot analysis was performed as previously reported [10,15]. Densitometric analysis of the bands and quantitation to β-actin was carried out (BioRad GS-800 calibrated densitometer; Hercules, CA). The following antibodies were used: anti-PPARγ raised against the C-terminus of the protein (sc-7273), anti-p21 (sc-6246), anti-cyclin D1 (sc-718), anti-PTEN (sc-7974) (Santa Cruz Biotechnology, Santa Cruz, CA); anti-COX-2 (1160112), anti-iNOS (160862) (Cayman Chemical Co., Ann Arbor, MI) anti-$p27^{kip1}$ (610241), anti-E-cadherin (610405) (BD Transduction Laboratories, Lexington, KY) anti-FLAG M2 (F3165), anti-β-actin (A5441) (Sigma-Aldrich, St. Louis, MO).

2.8. Loss of heterozygosity analysis

Loss of heterozygosity (LOH) was assessed as described, using the microsatellite markers D31259 and D3S3701, which flank *PPARG* [16]. Briefly, 100 ng of DNA extracted from colorectal cancers, polyps and matched normal mucosa was PCR amplified and the PCR products were separated on 6% SDS-PAGE. The allele size and relative intensity were determined by densitometry (BioRad GS-800 calibrated densitometer, Hercules, CA) and analyzed by GeneMapper software version

3.7 (Applied Biosystem, Foster City, CA). The assays were repeated three times in independent experiments with different DNA preparation. Each allele was scored by comparing the ratio of the signal intensity between the tumor (T) and its corresponding normal tissue (N). LOH was confirmed if a tumor allele showed at least a 50% reduction in intensity in tumor tissue with respect to the matched normal DNA.

2.9. Immunohistochemistry and immunofluorescence analysis

Immunohistochemical analysis on tumors, transitional mucosa (TM) and distant non-neoplastic mucosa was performed as described [15]. The antibodies used were: anti-PPARγ (C-terminus) (sc-7273) (Santa Cruz Biotechnology, Santa Cruz, CA); anti-β-catenin (610153) anti-E-cadherin (610405) (BD Transduction Laboratories, Lexington, KY); anti-COX-2 (1160112) (Cayman Chemical Co., Ann Arbor, MI); anti-CD68 (KP-1) and anti-Ki-67 (30-9) (Ventana Medical Systems, Tucson, AZ). The brown-stained colour by DAB chromogen was defined as positive reactivity, and evaluation of staining was made in a semi-quantitative manner by two independent investigators [15]. LoVo cells were used for immunofluorescence analysis; they were plated on coversplips and transfected with the various expression vectors with Lipofectamine 2000 (Invitrogen, Carlsbad, CA). Coverslips were washed with PBS, PFA fixed, permeabilized with Triton X-100, and incubated 1 h with PBS containing 1% vol/vol BSA. The fixed cells were then stained with anti-FLAG antibodies and revealed with FITC-conjugated anti-mouse IgG (Sigma-Aldrich, St. Louis, MO). Nuclei were stained with Hoechst 33258 (Sigma-Aldrich, St. Louis, MO). Images were generated with an Axiophot fluorescent microscope (Carl Zeiss, Milan, Italy) using 40× and 63× objectives. Images were processed using KS300 software (Carl Zeiss, Milan, Italy).

2.10. Statistical analysis

For all the experiments reported, data are expressed as mean ± S.D. and are obtained from at least five independent experiments performed in duplicate. Differences were assessed by the Student's *t* or Mann–Whitney test and considered to be statistically significant with a P value ≤ 0.05.

3. Results

3.1. Identification of a novel PPARγ mutation in colorectal cancer

To determine whether PPARγ plays any role in the pathogenesis of colorectal cancer, we screened a series of fifty sporadic tumors, selected on the basis of patients' personal and familial history, absence of such gene mutations as *APC*, or *PPARG* altered levels of expression [10,17]. To search for mutations along the entire *PPARG*, we extracted total RNA from tumor tissues, reverse transcribed and PCR amplified using as primers oligonucleotides derived from exons 1 and 3, 2 and 6, respectively, of the mature PPARγ1 mRNA [10]. The amplified bands were automatically sequenced: in a single patient we detected a heterozygous 866C>G transversion in exon 5. We then searched for the mutation directly on the DNA extracted from tumor tissue and peripheral blood lymphocytes, by amplifying *PPARG* exon 5 and sequencing the amplified product. The same heterozygous transversion was found in both DNAs, indicating that the mutation is germline transmitted. We ruled out the possibility that the base pair change found was a DNA polymorphism, because the analysis of more than 100 chromosomes from healthy individuals did not show the same DNA variation (data not shown).

The mutation causes a serine to cysteine substitution at position 289 (S289C) of the mature PPARγ1 protein (position S317C of PPARγ2) (Supp. Fig. S1A). Sequence comparison of this region of the ligand binding pocket reveals a remarkable amino acid identity across species as distant as *Xenopus laevis* and *Homo sapiens* (Supp. Fig. S1B). This striking conservation is likely due to the fact that these amino acids contribute to the ligand pocket formation and expose side-chain groups to establish and stabilize ligand–receptor interactions. Among these conserved amino acids, residues 285, 288, 289 and 290 are invariant in all species analyzed; interestingly, residues 288, 289 and 290 have been reportedly mutated. In particular, mutation P288H is associated with sporadic colorectal cancers [6]; V290M is a germline mutation found in a family with early onset type 2 diabetes and metabolic syndrome [11,12]; the S289C mutation is reported in this study. Thus, these three amino acids represent a *PPARG* mutational hot spot.

3.2. Clinical findings

The index case, *individual I-1*, an 80-year-old woman, underwent surgery for a newly diagnosed colorectal cancer localized at the proximal colon that was classified as a moderately differentiated adenocarcinoma by histological examination. Lymph nodes along the entire large intestine were invaded and distant metastases detected only in the liver. The proband referred repeated episodes of abdominal pain and intestinal dysfunction, occurring for many years before tumor onset. She also referred long-standing lipid metabolism derangements associated to a high BMI and hypertension accompanied by normal blood glucose and insulin levels (Table 1). She underwent chemotherapy following conventional protocols, which ensured steady general conditions with an acceptable standard of life for 3 years. CT scan and other tests, repeatedly carried out during the follow up, did not show involvement of other organs but liver, besides persistent blood lipid abnormalities. She died at the age of 83 because of massive liver metastases. Since the mutation is germline transmitted, all available family members were analyzed, after having given written informed consent (Fig. 1). The clinical and biochemical findings along with the mutation status of the tested family members are summarized in Table 1. *Individual II-1*, tested negative, does not show lipid metabolism alterations or overweight. In 2006, a control colonoscopy ruled out the presence of large intestine lesions. *Individual II-2*, tested positive, has elevated blood cholesterol and LDL cholesterol. In 2004, because of a painful intestinal dysfunction, she underwent colonoscopy and an aberrant crypt focus in the right colon was identified and removed. Four years later, she developed in the same location a dysplastic polyp removed during colonoscopy. Of the two children, *individual III-2*, tested negative, presents no dyslipidemia nor large intestine lesions as assessed by a control colonoscopy, whereas *individual III-3*, lean and apparently in good health, refuses any laboratory and genetic test. *Individual II-3*, tested positive, presents similar blood lipid abnormalities with normal glucose and insulin levels. In 2002, because of repeated episodes of abdominal pain associated to intestinal dysfunction, he underwent colonoscopy that evidenced three dysplastic polyps in the left colon that were endoscopically removed. A subsequent control colonoscopy was negative for polyps in the same and other locations. Of the two children, *individual III-5*, tested positive and has an altered lipid profile with no intestinal malfunctioning, probably due to the young age. In contrast, *individual III-4*, tested negative and has no lipid or metabolic alterations. *Individual II-4*, positive for the mutation, has blood lipid abnormalities with normal glucose level. In 2005, because of abdominal pain and intestinal dysfunction, she underwent colonoscopy that evidenced a polyp in the distal colon that was endoscopically removed. Of the two daughters, *individual III-6*, negative for the mutation, has no blood abnormalities or intestinal dysfunction, while *individual III-7* refuses any testing.

The analysis of the present family reveals that the S289C mutation is germline transmitted. The proband exhibited a profile of altered lipid metabolism associated with some features of the metabolic syndrome. However, all tested mutation carriers display a variable

Table 1
Clinical and biochemical characteristics of the family members tested for the mutation.

Family members										
Parameters	I_1	II_1	II_2	II_3	II_4	III_2	III_4	III_5	III_6	Reference values
PPARG status [a]	866C>G	wt	866C>G	866C>G	866C>G	wt	wt	866C>G	wt	
Gender	F	M	F	M	F	F	M	F	F	
Age (at presentation)	83* (80)	62 (57)	59 (54)	55 (50)	59 (53)	39 (34)	26 (21)	18 (14)	30 (25)	
BMI [b]	34.5	22	37.1	25	29	23	26	26	23	BMI>30 kg/m^2 obese
Glucose	106	80	80	95	95	93	75	91	104	75–110 mg/dl
Insulin	5.3	6	3	4	5	8	4	5	15	2–25 U/l
Impaired glucose tolerance [c]	A	A	A	A	A	A	A	A	A	P/A
Cholesterol	293	176	270	280	210	180	110	210	170	7–200 mg/dl
HDL cholesterol	79	60	83	75	65	95	85	80	70	>45 mg/dl
LDL cholesterol	196	140	160	210	170	122	90	150	130	0–150 mg/dl
Triglycerides	193	135	103	130	140	125	100	120	120	50–150 mg/dl
Hypertension	P	A	A	A	A	A	A	A	A	P/A
Large intestine polyps [d]	0	0	2	3	1	0	0	0	0	0

Age refers to the current age and in parenthesis that at presentation; Abbreviations: P/A indicates Presence/Absence.
[a] Nucleotide numbering reflects cDNA numbering with +1 corresponding to the A of ATG translation initiation codon in the reference sequence (NM_138712.3). The initiation codon is codon 1.
[b] Body mass index (BMI).
[c] Blood glucose levels measured 2 h after an oral glucose solution administration was <140 mg/dl (<7.8 mmol/l) in all individuals analyzed.
[d] Reports the results of a control colonoscopy carried out to show the presence/absence of relevant large intestine alterations in family members over 30 years old.
* Denotes a deceased patient.

profile of dyslipidemia with normal blood glucose, insulin levels and insulin sensitivity (Table 1). The occurrence of other metabolic diseases was ruled out on the basis of blood and clinical tests (data not shown). Interestingly, family members bearing the mutation present within their fourth–fifth decade of life intestinal polyps that presumably can evolve to a full-blown neoplasia, as conceivably occurred in the index case. The detection of polyps exclusively in positive-tested family members suggests that the S289C mutation is transmitted as a dominant trait.

3.3. In vitro expression and transcriptional activity of PPARγ and S289C and V290M mutants

In order to study the expression of the S289C mutant in an in vitro system, we transiently transfected the expression vectors containing the tagged PPARγ, S289C and V290M cDNAs into Cos7 cells (Supp. Fig. S2A). Using the anti-FLAG antibody we detected a specific band of about 64 kDa only in extracts from transfected cells. The intensity of the wild type band was equivalent to the mutant bands, as determined after normalization for transfection efficiency (Supp. Fig. S2B).

To evaluate the transactivation capacity of wild type PPARγ, S289C and V290M mutants, Cos7 cells were cotransfected with the expression vectors carrying the corresponding cDNAs and a reporter gene (Fig. 2). This construct contains three copies of a Peroxisome Proliferator Response Element (PPRE) fused upstream to the minimal herpes simplex thymidine kinase (TK) promoter that in turn drives transcription of a luciferase reporter gene [10]. The cells were transfected for 24 h and exposed to increasing concentrations of troglitazone, a selective agonist, member of the tiazolidinedione family of antidiabetic drugs.

In PPARγ-transfected cells, we observed a strong ligand-dependent transcriptional response, whereas in cells transfected with the S289C and V290M mutants we observed a negligible response, even at the highest ligand concentrations used. Indeed, in S289C mutant-transfected cells we detected an even lower (~50%) luciferase activity than in cells transfected with the empty expression vector, which probably reflects inhibition of the endogenous receptor (Fig. 2A, inset) [11,12]. We also transfected Cos7 cells with the PPRE-TK-luciferase reporter gene and increasing amounts of PPARγ or mutant expression vectors, in the presence of a fixed concentration of the ligand (1 μM troglitazone). PPARγ caused a proportional increase of luciferase activity, whereas the mutants did not, even at the highest ratios used (Fig. 2B). Similar effects were obtained with other PPARγ agonists such as: pioglitazone, rosiglitazone and 15-prostaglandin J2 (15-PGJ2) (data not shown). Therefore, the S289C mutant does not promote

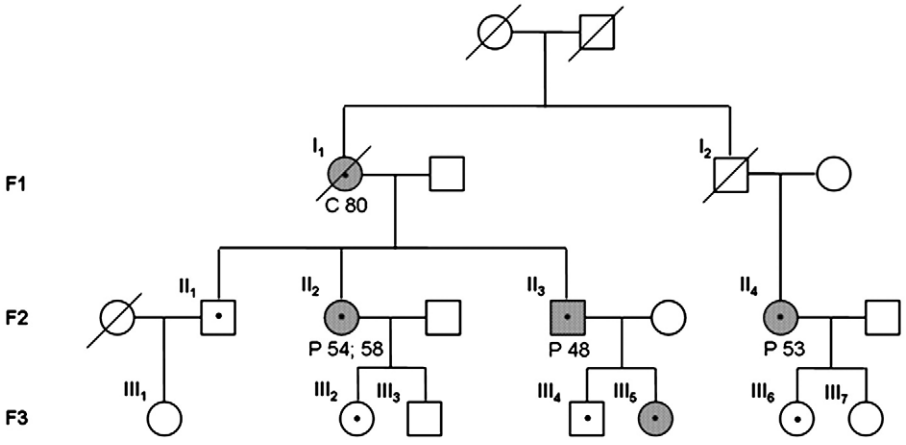

Fig. 1. Patient pedigree shows the distribution of the S289C germline mutation in family members. Dots indicate individuals tested for the mutation; filled symbols mutation carriers; crossed symbols deceased individuals; P and C denote the age at diagnosis of individuals bearing large intestine polyps or carcinoma, respectively.

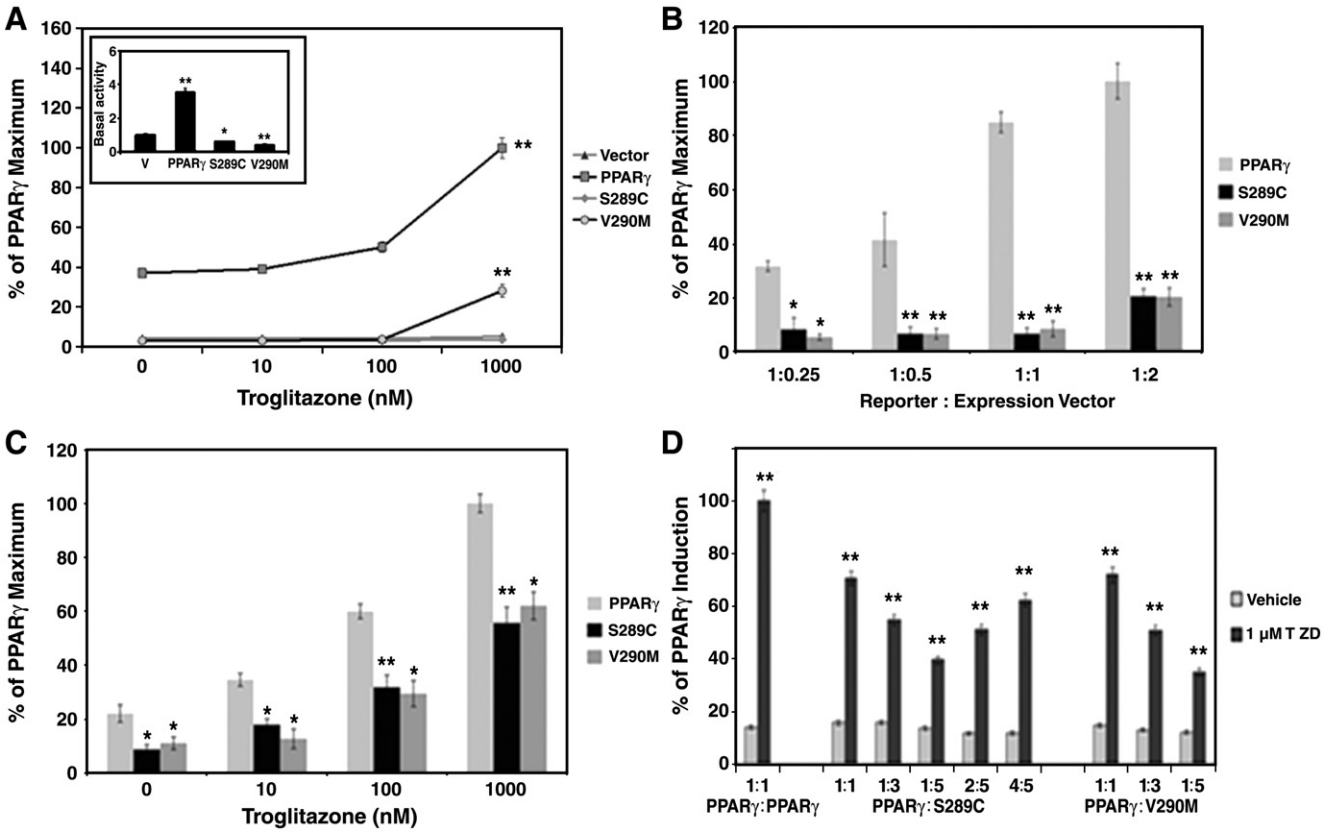

Fig. 2. S289C and V290M mutants have impaired transactivation ability and interfere with PPARγ function. (A) S289C and V290M do not activate a reporter gene. Cos7 cells were transfected with the PPRE-TK-luciferase reporter gene and PPARγ (■), S289C (▲), V290M (●) expression vectors or the empty vector (◆), in the presence of increasing concentrations of troglitazone. Transcriptional activity is reported relative to the maximum obtained with PPARγ. Inset: basal transcriptional activity (see text). (B) Cos7 cells exposed to a single dose of troglitazone were transfected with the reporter gene and increasing amounts of PPARγ (light grey), S289C (black) or V290M (dark grey) expression vectors. The reporter/expression vector ratios used are indicated, whereas the transactivation activity is reported relative to the maximum (100%) obtained with PPARγ receptor. (C) Both mutants interfere with the transactivation activity of PPARγ. The reporter gene was cotransfected with equal amounts of PPARγ and S289C (black) or V290M (dark grey) expression vectors (ratio1:1) or with PPARγ expression vector alone (light grey) in Cos7 cells exposed to increasing concentrations of troglitazone as indicated. Transcriptional repression is reported relative to the maximal activation obtained with PPARγ receptor. (D) Cos7 cells, exposed to vehicle or troglitazone, were cotransfected with the reporter gene and a fixed amount of PPARγ and increasing concentrations of S289C or V290M expression vectors. Re-addition of the wild type PPARγ expression vector recovered transcriptional activity (lanes indicated as 2:5 and 4:5). Transcriptional repression is reported relative to the maximal activation obtained with PPARγ expression vector alone. The CMV β-galactosidase control plasmid was added to each cotransfection to normalize for different transfection efficiency. Results are the mean ± S.D. of at least five independent experiments, each performed in duplicate. The *P* value was calculated for each panel by the Student's *t* test. $^{*}P \leq 0.05$; $^{**}P < 0.01$ compared to the corresponding controls. Abbreviation: V = empty vector.

transcription from a reporter gene, as the V290M mutant. To investigate the possibility that the S289C mutant could interfere with PPARγ activity, we cotransfected Cos7 cells with the PPRE-TK-luciferase reporter gene and equal amounts of PPARγ and S289C expression vectors (ratio 1:1) in the presence of increasing concentrations of troglitazone. At all ligand concentrations, luciferase activity was markedly lower (~60% of the PPARγ-induced response) than reporter gene cotransfected with PPARγ expression vector alone; at the basal level, only minimal differences were instead observed (Fig. 2C). A similar degree of interference has been reported for previously described *PPARG* mutants, such as V290M, and attributed to a dominant negative mode of action [11,12]. Indeed, in the same experimental conditions, the V290M mutant reduced wild type activity as the S289C mutant (Fig. 2C). We also tested S289C and V290M mutants' ability to inhibit wild type PPARγ in cells transfected with fixed amounts of the reporter gene and PPARγ expression vector along with increasing concentrations of S289C or V290M cDNA containing vectors. Addition of the mutants proportionally reduced luciferase activity, whereas re-addition of the wild type receptor reverted the inhibition observed, suggesting that the mutant receptor can be titrated out (Fig. 2D). These experiments demonstrate that the S289C mutant interferes with the transactivation properties of PPARγ in a ligand-dependent manner.

3.4. Growth inhibitory effects of PPARγ and S289C mutant

We wondered whether the S289C mutant retains the ability of the wild type receptor to inhibit cell growth [8,18,19]. To address this issue, we used the colony-forming efficiency assay [13] using NIH-3T3 cells as recipients because they express PPARγ at levels below the detectable threshold of the currently available methods. PPARγ reduced colony-forming efficiency by about 50% with respect to the cells transfected with the empty vector alone. The S289C mutant, on the contrary, increased this value by about 50% compared to the control (Fig. 3A). These experiments indicate that PPARγ inhibits cell growth, while S289C has lost this property. To determine the impact of the mutant on cell proliferation, we examined BrdUrd incorporation in cells transiently expressing PPARγ or the S289C mutant constructs [14]. PPARγ reduced cell proliferation by about 50% (15% vs. 28%), whereas, surprisingly, the S289C mutant increased BrdUrd incorporation with respect to the control (58% vs. 28%) (Fig. 3B). These experiments suggest that the S289C mutant has lost growth suppression properties.

3.5. The S289C mutant affects target genes expression in vivo

To examine the effects of the S289C mutation on PPARγ activity and target genes expression in vivo, we measured its protein levels on

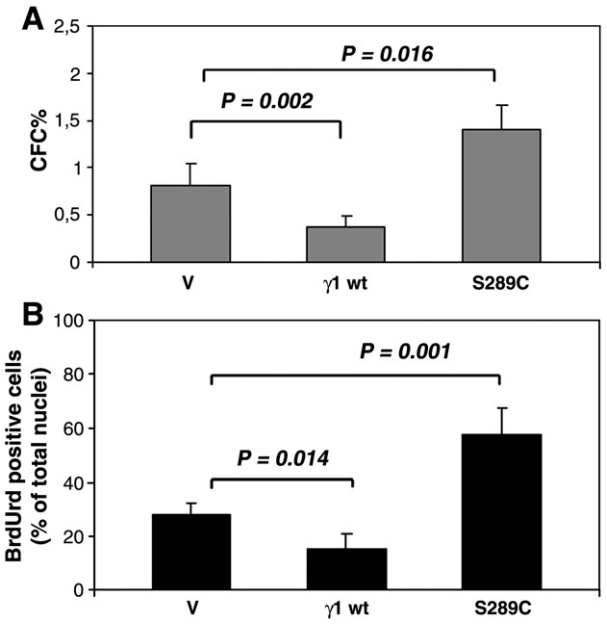

Fig. 3. S289C and V290M mutants affect PPARγ growth inhibitory ability in vitro. (A) A colony-forming efficiency assay was performed in NIH-3T3 transfected with the indicated expression vectors (see Section 2). (B) Percentage of BrdUrd incorporating NIH-3T3 cells transfected with the various expression vectors. The histograms represent the mean ± S.D. of five independent experiments, each performed in duplicate. The *P* value reported in each graph was obtained by the Mann–Whitney test. Abbreviation: V = empty vector.

extracts from tumor samples and matched adjacent mucosa. The analysis included several specimens on the basis of absence of *PPARG* mutations, availability of tissue samples and PPARγ expression levels. Among the PPARγ target genes, we investigated PTEN and E-cadherin, both tumor suppressor genes [20,21], and report representative results on samples with high (2 N–2 T and 3 N–3 T) or low (4 N–4 T) PPARγ levels, respectively. In the proband, PPARγ showed equivalent expression in both tissues. PTEN and E-cadherin declined from the normal mucosa to the tumor, reflecting PPARγ activity. In patients 2 and 3 PPARγ expression was higher in tumor than the adjacent mucosa [22] similarly to PTEN and E-cadherin. PPARγ was low in both tissues of patient 4 (Fig. 4A), paralleling PTEN and E-cadherin (Fig. 4B). The expression of several *PPARG* target genes, such as p27, p21 and Cyclin D1, mirrored that of PTEN and E-cadherin and was strictly related to PPARγ expression and activity (data not shown). Similar results were also obtained in transfections of human colon carcinoma cells in culture with the wild type and mutant *PPARG* expression vectors (HT29 cells, our data not shown). All together these data demonstrate that the S289C mutant no longer transactivates target genes in vivo, reproducing the results obtained in vitro.

3.6. PPARG LOH analysis

To establish whether a somatic "second hit" has occurred in the proband's tumor tissues, leading to inactivation of the *PPARG* wild type allele, we performed LOH analysis, using two microsatellite markers flanking the 5′ and 3′ ends of the gene [16]. We did not detect allelic loss in tumor tissues as compared to the normal mucosa (Fig. 4, panel C). Similarly, no LOH was detected in the adenoma of individual II-2 bearing the mutation (data not shown). We did not detect *PPARG* LOH also in a subset of sporadic colorectal cancers with reduced PPARγ expression (Fig. 4, panel C), suggesting that epigenetic mechanisms could play an important role in *PPARG* inactivation (our unpublished data).

3.7. Anti-inflammatory and anti-proliferative potential of wild type and S289C PPARγ mutant in vivo

PPARγ interferes with the expression of pro-inflammatory genes, a process termed transrepression [23]. To verify whether our mutant still exerts this function, we monitored COX-2 and iNOS protein levels on extracts from the same tumor specimens and matched adjacent mucosa reported above. In the proband, COX-2 and iNOS were unexpectedly expressed in the normal mucosa and their levels increased in the tumor. In patients 2 and 3, their expression was instead very low. In patient 4, COX-2 and iNOS were higher in the tumor than the normal mucosa (Fig. 4A and B). As in the proband's tissues these protein levels were in an inverse relation with PPARγ activity, we suggest that the mutant receptor no longer impedes the activation of inflammatory genes. To exploit the possibility that S289C could also affect the proliferation rate of colonic cells and counteract the inflammatory immune response, we analyzed the same tumor tissues and the paired transitional mucosa by immunohistochemistry for Ki-67 and CD68, markers of cell proliferation and elicited immune response, respectively [24,25]. In the proband's normal mucosa, the staminal cells and those undergoing proliferation at the lower third along the longitudinal axis of each crypt showed positivity for Ki-67 antibody (Fig. 5, panel a). In the transitional mucosa, i.e. the normal matched mucosa more proximal (only 3 cm away) to the tumor [26], Ki-67 positive cells were unexpectedly higher and distributed along the entire longitudinal axis (panel b). They further increased in tumor sections, where the crypts were no longer recognizable (panel c). In the same samples, CD68 infiltration proportionally increased from the normal to the transitional mucosa up to the tumor (panels d–f). In patient 2's sections, the few Ki-67 positive cells showed no differences in the distribution between the normal and transitional mucosa; they slightly increased only in the tumor (panels g–i). A similar staining pattern was obtained with the anti-CD68 antibody (panels j–l). The increased number of the Ki-67 positive cells in the proband's transitional mucosa suggests that they may have a higher proliferative potential. To verify this hypothesis, we analyzed bioptic specimens from a mutation carrier, individual II-2 (see Table 1), who developed subsequent lesions in the proximal colon in the last few years (Supp. Fig. S3). The first specimen (P1, panels b1–b3) evidenced an aberrant crypt focus characterized by a far higher number of Ki-67 and CD68 positive cells than the normal mucosa (NM, panels a1–a3). Interestingly, 4 years later, she developed a dysplastic polyp in the same location with a more pronounced inflammation and an even higher number of Ki-67 positive cells (P2, panels c1–c3).

All together, the data demonstrate that the S289C mutant is greatly impaired in activating target genes, in repressing the inflammatory response and in blocking cell proliferation also in vivo. In addition, the expression profile detected was very different from that observed in unrelated sporadic and FAP polyps (Supp. Table 1). These we believe may represent the first events that trigger tumorigenesis, as suggested by the data obtained on tissue specimens from a mutation carrier. In fact, an aberrant crypt focus can evolve to a dysplastic polyp and, eventually, to a frank carcinoma if not properly diagnosed and surgically removed. This series of alterations may conceivably have occurred also in the proband.

3.8. Putative effects of the S289C mutation on the structure of the PPARγ ligand binding domain

To elucidate the structural basis of the deleterious effects of the S289C mutation, we examined the crystal structure of both unbound and ligand-bound form of PPARγ ligand binding domain (PDB code 1PRG and 1FM9, respectively). This domain consists of 12 α-helices and 4 small β-strands that fold to generate a large hydrophobic cavity in the form of a helical sandwich where the ligand accommodates

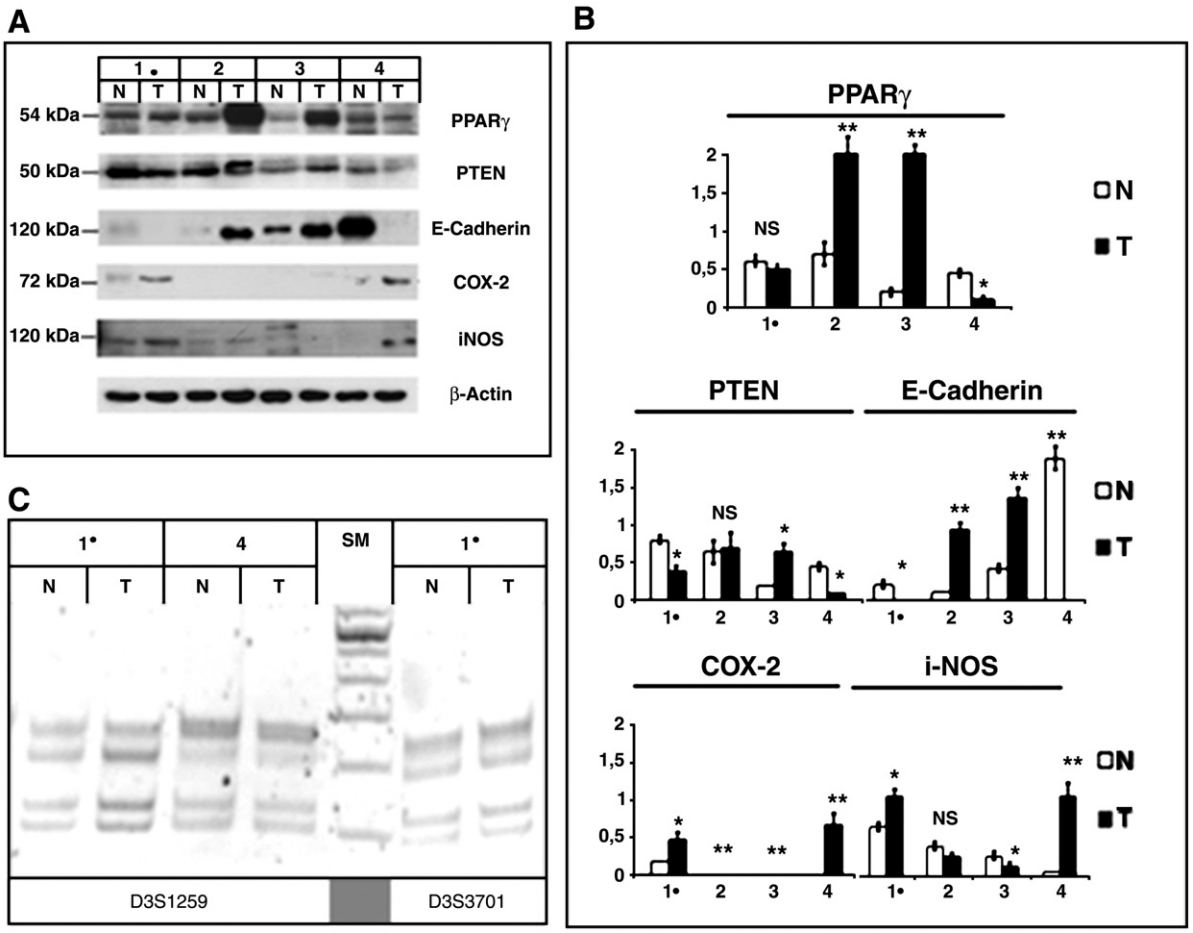

Fig. 4. PPARγ and target gene expression in vivo and LOH analysis. (A) Protein extracts from tumor tissues (T) and matched adjacent mucosa (N) were analyzed by Western blot, using the antibodies raised against the proteins indicated on the side. Panels illustrate the results obtained with the proband (1*) and some representative samples (from 2 to 4), as indicated in the text. The m.w. of the proteins investigated are also illustrated. (B) The histograms report the quantitation obtained after densitometric scanning of the bands referred to β-actin as internal control. Results are reported as mean ± S. D. of at least five independent experiments. The *P* value was calculated for each panel by the Student's *t* test. $^{*}P \leq 0.05$; $^{**}P < 0.01$ compared to the corresponding control tissues. Abbreviation: NS = not significant. (C). LOH assay. Both microsatellite loci flanking *PPARγ* were retained in the tumor tissue of the proband (1*) as compared to the normal mucosa. No LOH was observed in unrelated tumor samples with low PPARγ expression levels.

(Fig. 6A) [27,28]. Helix 3, where serine 289 resides, forms the inner part of the pocket together with helices 2 and 4. When a TZD ligand is present, the Ser289-OH group forms a direct hydrogen bond with the head group of the agonist (rosiglitazone in this case), stabilizing receptor–ligand interactions. The replacement of the serine with a cysteine residue should not impede the entry and positioning of the agonist, because the size of the cysteine side-chain is similar to that of the serine and should not impair the formation of a weak hydrogen bond by means of the SH group (Fig. 6A). Our data, however, indicate that the transactivation potential of the mutant is dramatically hampered and is not reverted by the ligand. Other reasons should be taken into account to explain the low affinity of the mutant protein

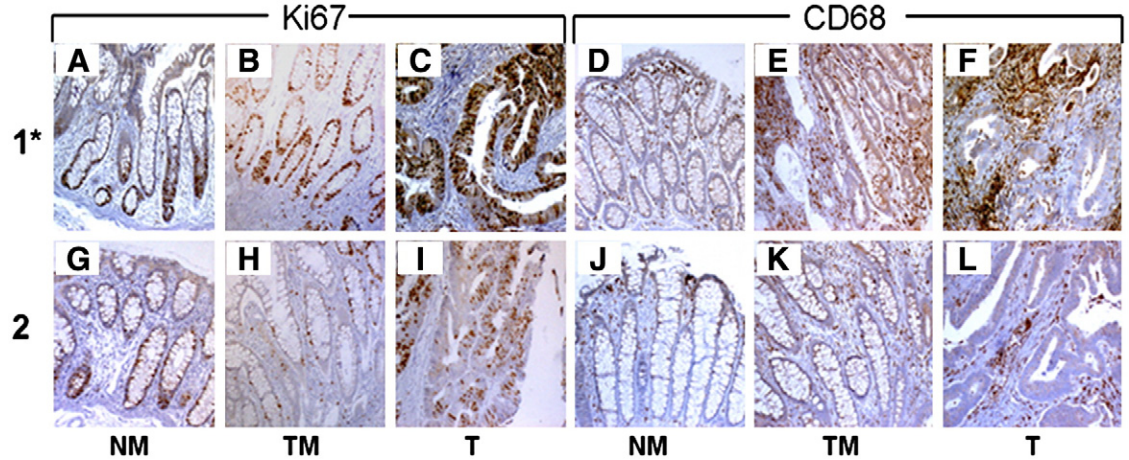

Fig. 5. Ki-67 and CD68 immunohistochemical analysis of tumor samples from the proband and an unrelated patient. (A) The analysis was carried out on 4 μm tick sections of the adjacent normal mucosa (NM), transitional mucosa (TM) and tumor mass (T) from the proband (1*) and individual 2, expressing high levels of wild type PPARγ.

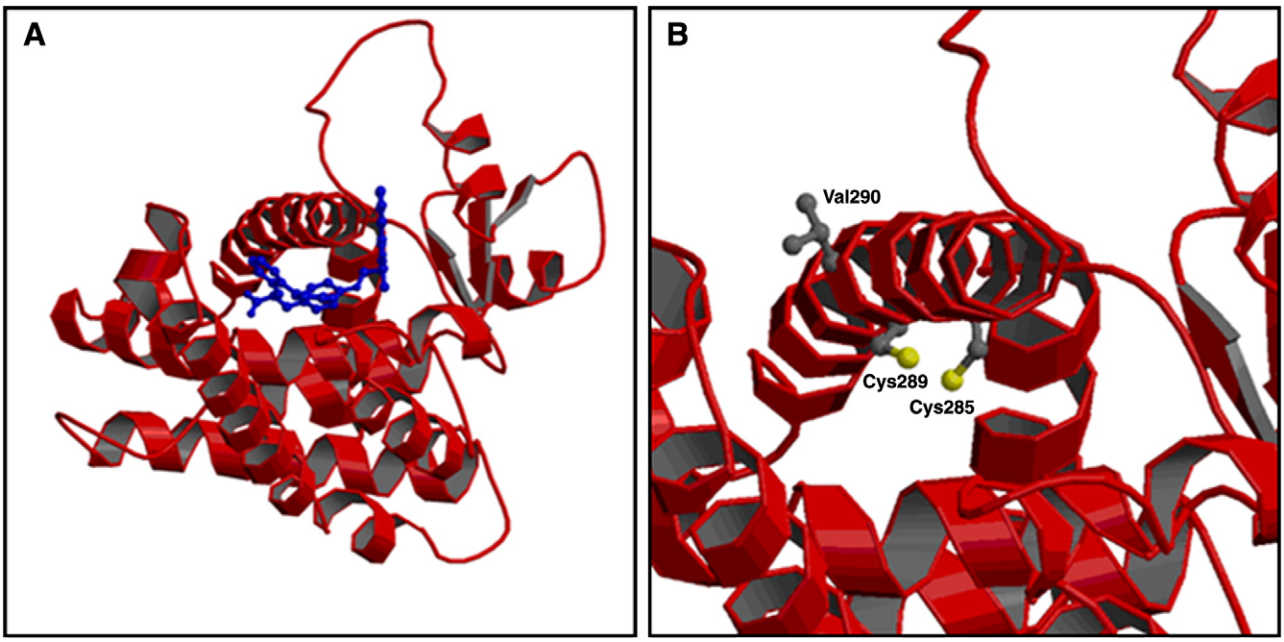

Fig. 6. Effects of the S289C mutation on the structure of the ligand binding pocket. (A). Ribbon representation of PPARγ fold. The rosiglitazone ligand is drawn in ball-and-stick representation and coloured in blue. (B) Enlargement of the PPARγ ligand binding region. Cys285, Cys289 and Val290 are drawn in ball-and-stick representation. The relative orientation of the V290 and S289 with respect to the α helix structure is reported, as well as the relative position and vicinity of the two SH groups (285 and 289). The figures were prepared with MOLSCRIPT.

for the agonist. The S289C mutation could affect the conformation of helix 3 that, upon binding, becomes packed against helix 12, providing the "lid" in the mouse trap model of receptor-agonist binding [27,28]. Moreover, the folding back of helix 12 causes the exposure of the LXXLL motif involved in coactivator recruitment. A perturbation in the interaction between helix 3 and helix 12 could, thus, significantly affect receptor functions. This is indeed modified when valine 290 is replaced with methionine. The relative orientation of these two helices is changed, compromising both receptor-ligand binding and -coactivator recruitment [11]. Ser289, in contrast, has a different orientation, which lines the binding pocket for the ligand, so that the S289C mutation should not affect the interaction between helix 3 and helix 12 [27,28] (Fig. 6A). Inspection of the region surrounding S289 suggests another intriguing possibility. It is, in fact, tempting to speculate that the mutant S289C could form a disulphide bridge with the nearby residue C285 (Fig. 6B). The C_α–C_α distance between these two residues is indeed in the range of the most common distances between two C_α of cysteines involved in disulphide bridges [29]. Moreover, in a significant number of cases, three amino acid residues separate the two cysteines involved in disulphide bridges as in the case reported here [29,30]. The formation of such a bridge in the binding pocket would render sterically impossible the entrance of the agonist (i.e. the presence of a rigid covalent link between C285 and C289 would entirely modify the size and shape of the binding pocket). This seems to be a reliable structural explanation of the biological effects caused by the S289C mutation.

3.9. Subcellular localization of the S289C mutant in vitro and in vivo

In order to get further information on the subcellular localization of PPARγ and its mutants, we transiently transfected the PPARγ, S289C and V290M cDNAs containing expression vectors into human colorectal cancer cells (LoVo) and detected the resulting proteins by immunofluorescence with an anti-FLAG antibody (Supp. Fig. S4A). In the absence of ligand, the wild type receptor showed a diffuse cytosolic staining with some positive nuclei (panels a–a1). In contrast, both mutants were distributed exclusively into the cytosol (panels b through c1). Upon troglitazone addition, PPARγ showed a marked nuclear positivity, (panels e–e1) whereas the S289C mutant a persistent cytosolic staining (panels b–b1) and the V290M mutant only a marginal translocation to the nucleus (panels g–g1). We investigated PPARγ localization in vivo on tissue sections from the proband and other selected patients (Supp. Fig. S4B). In the normal mucosa, PPARγ was mainly in the cytosol of cells located at the tip of the crypts, indicating that it is expressed in fully differentiated cells (panel a1). In the tumor, PPARγ staining was still confined to the cytosol (panel a2). In patient 2's normal mucosa, PPARγ was predominantly nuclear (panel b1); in the tumor, a stronger positivity was detected and distributed between the cytosol and the nucleus (panel b2). These data indicate that PPARγ shuttles between the cytosol and nucleus and addition of the ligand triggers nuclear translocation. This occurs only partially for the V290M mutant as it can weakly bind the ligand and restores some biological activities [11]. The S289C mutant, in contrast, retains a steady and exclusive cytosolic distribution, probably because it cannot bind the ligand. This impairment could explain its subcellular localization and at least some of the results obtained.

4. Discussion

Nuclear receptors play important roles in the establishment and maintenance of whole-body homeostasis. They, in fact, respond to several nutritional or exogenous compounds and, at the same time, control the expression of a variety of genes that regulate a vast array of metabolic pathways. Among nuclear receptors, PPARs are master regulators of energy, lipid and carbohydrate metabolism. PPARγ, in addition, modulates differentiation of several epithelial cells, especially those of the gastro-intestinal tract where it also contributes to the control of local inflammatory processes [31]. Coherent with these functions, changes in PPARγ activity have been related to an altered differentiation process and hence to proliferation and tumorigenesis. Contrasting reports in the literature, however, have raised the question whether PPARγ acts as tumor suppressor or stimulates tumor formation. We report here a novel heterozygous *PPARG* germline mutation (c.866C>G) in exon 5, that replaces the amino acid serine with cysteine (S289C). The mutant has impaired transactivation

potential in vitro and acts as dominant negative to the wild type receptor, as many *PPARG* loss-of-function mutants previously described [5]. Strikingly, the base pair change is found in a patient affected by colorectal cancer in the proximal colon that invaded lymph nodes of the entire intestine and produced metastases to the liver. We exclude that such an association is merely accidental due to the age of the patient, as a survey of all available family members shows that only mutation carriers develop specific lesions of the large intestine in their fourth–fifth decades of life (Fig. 1 and Table 1). In fact, bioptic specimens from a mutation carrier show an aberrant crypt focus, the earliest lesion that initiates colon tumorigenesis, subsequently followed in the same location by a dysplastic adenomatous polyp with a higher transforming potential. At the molecular level, these alterations are characterized by a large number of Ki-67 and CD68 positive cells, documenting an enhanced proliferation rate and inflammatory immune response. Interestingly, both characteristics are already detected in the proband's transitional mucosa (Fig. 5), indicating that the mutant receptor confers a reduced ability to restrain cell growth. Our data further support the notion that PPARγ is a tumor suppressor. However, we could not detect loss of the wild type allele in tumor tissues by LOH analysis (Fig. 4C) or additional somatic mutations (data not shown) at odds with other tumor suppressors. *PPARG* somatic heterozygous mutations (E286P and R288H) have been reported in a series of colorectal cancers and the profound effects on receptor's activity have been invoked to explain the association to tumor development [6]. *PPARG* in vivo could behave either as a haploinsufficient or a dominant negative tumor suppressor gene, like *TP53*. [32–34]. However, preliminary data suggest that epigenetic events, such as promoter methylation and histone modifications, play an important role in the inactivation of the wild type allele (our unpublished data) [15].

This is the first *PPARG* germline mutation associated to the development of large intestine polyp that can putatively evolve to a full-blown carcinoma, although we do not know the exact frequency of *PPARG* mutations, especially those related to colorectal cancer [35].

Another relevant trait associated to the S289C mutation is the lipid metabolism derangement. The role that PPARγ plays as a master regulator of the intermediate metabolism, in adipose tissue differentiation and in skeletal muscle function may explain the systemic metabolic variations associated with previous *PPARG* mutations, such as type 2 diabetes, several features of the metabolic syndrome and partial lipodystrophy [2–5]. Our proband presented an altered lipid profile associated with obesity and hypertension without blood glucose and insulin levels, insulin sensitivity alterations, or lipodystrophy. Only mutation carriers and no other family members show different profiles of lipid derangement, likely due to a variable penetrance of the present mutation. In none of the tested individuals, however, did we detect elevated blood glucose and insulin levels, altered glucose tolerance test or other signs of type 2 diabetes (Table 1 and Fig.1). The lipid metabolism disturbances present in the S289C mutation carriers appear then to be distinct from glucose and insulin metabolism alterations. This is the first report of a *PPARG* mutation in humans lacking this association and the reasons for such a discrepancy are not known at the moment. Interestingly, mice harboring a heterozygous *Pparg* mutation P465L maintain normal glucose and insulin levels and display no insulin resistance and lipid abnormalities [36]. The equivalent mutation P467L in humans is characterized by type 2 diabetes, a severe insulin resistance and a fat distribution different from that found in mice bearing the same mutation [11,12]. These metabolic differences may be attributed to species-specific effects of the mutation. Recently, the same mutant mice have shown an increased proliferation rate of the neointimal cells that promotes atherosclerosis [37]. The lack of association with glucose metabolism alterations and the higher cell proliferation rate are similar to the features reported here for the S289C mutation. Finally, superimposing the S289C mutation to the X-rays crystal structure of the ligand binding domain suggests that the SH group generated by the mutation could interact with the close cysteine 285-SH group to form an S–S bridge. The covalent bond would stably reduce the depth of the binding pocket, impede the positioning of the ligand and could explain at least in part the biological effects detected.

In conclusion, we report the identification of a novel mutation located in a *PPARG* mutational hot spot. The S289C mutant is hampered in its transactivation and transrepression activity and no longer restrains cell growth. These molecular events may underlie the lesions found in the colonic mucosa of the mutation carriers and explain their possible evolution to a frank carcinoma. The mutation also affects the lipid profile without interfering with the glucose or insulin metabolism. The similarities and differences in the phenotype caused by the mutation described here as compared to previously reported mutations, provide an opportunity to further dissect the role of PPARγ in various aspects of cellular homeostasis as well as in the pathogenesis of metabolic diseases and colon tumorigenesis.

Acknowledgements

We wish to thank Jean Gilder for editing the text. We would like to thank Prof. Chatterjee for providing us the PPARγ mutant V290M-containing expression vector. This work is supported by grants from MIUR (FIRB 2001 and PRIN 2004) to VC.

Appendix A. Supplementary Data

Supplementary data associated with this article can be found, in the online version, at doi:10.1016/j.bbadis.2010.01.012.

References

[1] G.A. Francis, E. Fayard, F. Picard, J. Auwerx, Nuclear receptors and the control of metabolism, Ann. Rev. Physiol. 65 (2003) 261–311.
[2] B.M. Spiegelman, PPARγ: adipogenic regulator and thiazolidinedione receptor, Diabetes 47 (1998) 507–514.
[3] J.N. Feige, L. Gelman, L. Michalik, B. Desvergne, W. Wahli, From molecular action to physiological outputs: peroxisome proliferator-activated receptors are nuclear receptors at the crossroads of key cellular functions, Prog. Lipid Res. 45 (2006) 120–159.
[4] T.M. Willson, M.H. Lambert, S.A. Kliewer, Peroxisome proliferator-activated receptor γ and metabolic disease, Annu. Rev. Biochem. 70 (2001) 341–367.
[5] C. Knouff, J. Auwerx, Peroxisome proliferator-activated receptor-γ calls for activation in moderation: lessons from genetics and pharmacology, Endocr. Rev. 25 (2004) 899–918.
[6] P. Sarraf, E. Mueller, W.M. Smith, H.M. Wright, J.B. Kum, L.A. Aaltonen, A. de la Chapelle, B.M. Spiegelman, C. Eng, Loss-of-function mutations in PPARγ associated with human colon cancer, Mol Cell 3 (1999) 799–804.
[7] M. Ristow, D. Muller-Wieland, A. Pfeiffer, W. Krone, C.R. Kahn, Obesity associated with a mutation in a genetic regulator of adipocyte differentiation, N. Engl. J. Med. 339 (1998) 953–959.
[8] L. Michalik, B. Desvergne, W. Wahli, Peroxisome-proliferator-activated receptors and cancers: complex stories, Nat. Rev. Cancer 4 (2004) 61–70.
[9] C. Grommes, G. Landreth, M.T. Heneka, Antineoplastic effects of peroxisome proliferator activated receptor γ agonists, Lancet Oncol. 7 (2004) 419–429.
[10] L. Sabatino, A. Casamassimi, G. Peluso, M.V. Barone, D. Capaccio, C. Migliore, P. Monelli, A. Pedicini, A. Febbraro, A. Ciccodicola, V. Colantuoni, A novel peroxisome proliferator-activated receptor γ isoform with dominant negative activity generated by alternative splicing, J. Biol. Chem. 280 (2005) 26517–26525.
[11] I. Barroso, M. Gurnell, V.E. Crowley, M. Agostini, J.W. Schwabe, M.A. Soos, G.L. Maslen, T.D. Williams, H. Lewis, A.J. Schafer, V.K. Chatterjee, S. O'Rahilly, Dominant negative mutations in human PPARγ associated with severe insulin resistance, diabetes mellitus and hypertension, Nature 402 (1999) 880–883.
[12] D.B. Savage, G.D. Tan, C.L. Acerini, S.A. Jebb, M. Agostini, M. Gurnell, R.L. Williams, A.M. Umpleby, E.L. Thomas, J.D. Bell, A.K. Dixon, F. Dunne, R. Boiani, S. Cinti, A. Vidal-Puig, F. Karpe, V.K. Chatterjee, S. O'Rahilly, Human metabolic syndrome resulting from dominant-negative mutations in the nuclear receptor peroxisome proliferator-activated receptor γ, Diabetes 52 (2003) 910–917.
[13] F.A. Peverali, T. Ramqvist, R. Saffrich, R. Pepperkok, M.V. Barone, L. Philipson, Regulation of G1 progression by E2A and Id helix-loop-helix proteins, EMBO J. 13 (1994) 4291–4301.
[14] M.V. Barone, S.A. Courtneidge, Myc but not Fos rescue of PDGF signaling block caused by kinase-inactive Src, Nature 378 (1995) 509–512.
[15] M. Pancione, N. Forte, L. Sabatino, E. Tomaselli, D. Parente, A. Febbraro, V. Colantuoni, Reduced β-catenin and peroxisome proliferator-activated receptor γ expression levels are associated with colorectal cancer metastatic progression: correlation with tumor-associated macrophages, cyclooxygenase 2, and patient outcome, Hum. Pathol. 40 (2009) 714–725.

[16] J.J. Yeh, D.J. Marsh, J. Zedenius, T. Dwight, L. Delbridge, B.G. Robinson, C. Eng, Fine-structure deletion mapping of 10q22–24 identifies regions of loss of heterozygosity and suggests that sporadic follicular thyroid adenomas and follicular thyroid carcinomas develop along distinct neoplastic pathways, Genes Chromosomes Cancer 26 (1999) 322–328.
[17] K.W. Kinzler, B. Vogelstein, Lessons from hereditary colorectal cancer, Cell 87 (1996) 159–170.
[18] R.A. Gupta, P. Sarraf, E. Mueller, J.A. Brockman, J.J. Prusakiewicz, C. Eng, T.M. Willson, R.N. DuBois, Peroxisome proliferator-activated receptor γ mediated differentiation: a mutation in colon cancer cells reveals divergent and cell type-specific mechanisms, J. Biol. Chem. 278 (2003) 22669–22677.
[19] G.D. Girnun, W.M. Smith, S. Drori, P. Sarraf, E. Mueller, C. Eng, P. Nambiar, D.W. Rosenberg, R.T. Bronson, W. Edelmann, R. Kucherlapati, F.J. Gonzalez, B.M. Spiegelman, APC-dependent suppression of colon carcinogenesis by PPARγ, Proc. Natl. Acad. Sci. U.S.A. 99 (2002) 13771–13776.
[20] R.E. Teresi, C.W. Shaiu, C.S. Chen, V.K. Chatterjee, K.A. Waite, C. Eng, Increased PTEN expression due to transcriptional activation of PPARγ by lovastatin and rosiglitazone, Int. J. Cancer 118 (2006) 2390–2398.
[21] J.S. Annicotte, I. Iankova, S. Miard, V. Fritz, D. Sarruf, A. Abella, M.L. Berthe, D. Noël, A. Pillon, F. Iborra, et al., Peroxisome proliferator-activated receptor γ regulates E-cadherin expression and inhibits growth and invasion of prostate cancer, Mol. Cell. Biol. 26 (2006) 7561–7574.
[22] D. Wang, R.N. Dubois, Peroxisome proliferator-activated receptors and progression of colorectal cancer, PPAR Res (2008) 931074.
[23] G. Pascual, A.L. Fong, S. Ogawa, A. Gamliel, A.C. Li, V. Perissi, D.W. Rose, T.M. Willson, M.G. Rosenfeld, C.K. Glass, A SUMOylation-dependent pathway mediates transrepression of inflammatory response genes by PPARγ, Nature 437 (2005) 759–763.
[24] M.J. Iatropoulos, G.M. Williams, Proliferation markers, Exp. Toxicol. Pathol. 48 (1996) 175–181.
[25] A.M. Platt, A.M. Mowat, Mucosal macrophages and the regulation of immune responses in the intestine, Immunol. Lett. 119 (2008) 22–31.
[26] M. Mori, R. Shimono, Y. Adachi, H. Matsuda, H. Kuwano, K. Sugimachi, M. Ikeda, M. Saku, Transitional mucosa in human colorectal lesions, Dis. Colon Rectum 33 (1990) 498–501.
[27] R.T. Gampe Jr., V.G. Montana, M.H. Lambert, A.B. Miller, R.K. Bledsoe, M.V. Milburn, S.A. Kliever, T.M. Willson, E.H. Xu, Asymmetry in the PPARγ /RXRα crystal structure reveals the molecular basis of heterodimerization among nuclear receptors, Mol. Cell 5 (2000) 545–555.
[28] J. Uppenberg, C. Svensson, M. Jaki, G. Bertilsson, L. Jendeberg, A. Berkenstam, Crystal structure of the ligand binding domain of the human nuclear receptor PPARγ, J. Biol. Chem. 273 (1998) 31108–31112.
[29] M.T. Petersen, P.H. Jonson, S.B. Petersen, Amino acid neighbours and detailed conformational analysis of cysteines in proteins, Protein Eng. 12 (1999) 535–548.
[30] P.J. Kraulis, MOLSCRIPT: a program to produce both detailed and schematic plots of protein structures, J. Appl. Crystallogr. 24 (1991) 946–950.
[31] G. Rogler, Significance of anti-inflammatory effects of PPARγ agonists? Gut 55 (2006) 1067–1069.
[32] P. Alberici, C. Gaspar, P. Franken, M.M. Gorski, I. de Vries, R.J. Scott, A. Ristimäki, L.A. Aaltonen, R. Fodde, Smad4 haploinsufficiency: a matter of dosage, Pathogenetics 1 (2008) 2–12.
[33] C. Eng, K. Schneider, J.F. Fraumeni, F.P. Li, Third international workshop on collaborative interdisciplinary studies of *p53* and other predisposing genes in Li–Fraumeni syndrome, Cancer Epidemiol. Biomarkers Prev. 6 (1997) 379–383.
[34] A. Russell-Swetek, A.N. West, J.E. Mintern, J. Jenkins, C. Rodriguez-Galindo, R. Ribeiro, G.P. Zambetti, Identification of a novel TP53 germline mutation E285V in a rare case of paediatric adrenocortical carcinoma and choroid plexus carcinoma, J. Med. Genet. 45 (2008) 603–606.
[35] T. Ikezoe, C.W. Miller, S. Kawano, A. Heaney, E.A. Williamson, J. Hisatake, E. Green, W. Hofmann, H. Taguchi, H.P. Koeffler, Mutational analysis of the peroxisome proliferator-activated receptor gamma gene in human malignancies, Cancer Res. 61 (2001) 5307–5310.
[36] Y.S. Tsai, H.J. Kim, N. Takahashi, H.S. Kim, J.R. Hagaman, J.K. Kim, N. Maeda, Hypertension and abnormal fat distribution but not insulin resistance in mice with P465L PPARγ, J. Clin. Invest 114 (2004) 163–175.
[37] D. Meredith, M. Panchatcharam, S. Miriyala, Y.S. Tsai, A.J. Morris, N. Maeda, G.A. Stouffer, S.S. Smyth, Dominant-negative loss of PPARγ function enhances smooth muscle cell proliferation, migration, and vascular remodeling, Arterioscler. Thromb. Vasc. Biol. 29 (2009) 465–471.